Third International Conference on Inverse Design Concepts and Optimization in Engineering Sciences (ICIDES-III), Editor G.S. Dulikravich, Washington D.C., October 23-25, 1991

N92-13950

SUPERCRITICAL BLADE DESIGN ON STREAM SURFACES OF REVOLUTION WITH AN INVERSE METHOD

E. Schmidt, H.-D. Grein

Institut für Aerodynamik
und Gasdynamik
Universität Stuttgart
Pfaffenwaldring 21
D-7000 Stuttgart 80
FRG

p. 13

Abstract

The described method solves the inverse problem for supercritical blade-to-blade flow on stream surfaces of revolution with variable radius and variable stream surface thickness in a relative system. Some aspects of shockless design and of leading edge resolution in the numerical procedure are depicted. Some supercritical compressor cascades were designed and their complete flow field results were compared with computations of two different analysis methods.

Nomenclature

A	area
BN	blade number
La	Laval number
R	radius of stream surface
W	magnitude of velocity vector
d	profile thickness
h	stream surface thickness
l	profile chord length
m	meridional coordinate
s	arc length
t	cascade pitch
$\vec{w}$	velocity vector
x	chord coordinate
z	axial coordinate
Γ	circulation
Ω	axial velocity density ratio
θ	circumferential angle
β	flow angle
ε	inclination angle of stream surface
ρ	density
φ	potential function
ψ	stream function
ω	angular velocity

Subscripts:

1	upstream
2	downstream
BW	blade wake
SW	side wall
ax	axial
m	meridional
u	circumferential
Um	Transition

Third International Conference on Inverse Design Concepts and Optimization in Engineering Sciences
(ICIDES-III), Editor: G.S. Dulikravich, Washington D.C., October 23-25, 1991

INTRODUCTION

Increasing requirements on turbomachines concerning efficiency, compact construction and density of power lead to aerodynamically highly loaded blades. The admissible blade load and the profile losses are determined by the boundary layer development. High pressure ratios per stage and high turning of the flow increase the risk of boundary layer separation with the result of strongly growing losses. This problem is intensified by the risk of arising compression shocks. They are caused by the supercritical through-flow (with local supersonic regions), which is necessary for high mass flow density.

In regions with pressure rise, boundary layer separation can only be avoided by careful blade profiling for flow with minimum loss. In the past, turbomachinery bladings have mostly been designed with the aid of profile families. But in this way, depending on the plurality of parameters, a loss minimization is not possible. Especially in the transonic velocity region this procedure is insufficient since shockfree solutions can be found with only poor chances by iterative contour variation. In this region of maximum mass flow density very small variations of the geometry are connected with very high changes in the flow velocity. Therefore, it is convenient to prescribe the physical quantity, where the great changes appear, and to calculate the small but important variations of the geometry.

This alternative is given by inverse design: Starting from a prescribed shockfree velocity distribution, the corresponding profile contour is calculated numerically. By this means a perfect tailoring of the blade to the required turning problem is possible.

Up to now a perfect three-dimensional inverse design of flow fields in turbomachines is not executed since this problem is quite overdetermined. At present a standard procedure is to start a quasi three-dimensional computation by calculating the flow on meridional planes (S_2) by an analysis code (duct- or through-flow) to get the starting values of the calculation on several blade-to-blade planes (S_1) distributed along the blade height.

This multi-section design of the blade can be realized by inverse computation. The following inverse computation method is an extension of the former cylindrical version [1,2] to the design on stream surfaces of revolution with variable radius and variable stream surface thickness in a relative system. This development is a further step to approximate the real physical behaviour of the flow. The method is applied to the multi-section design of a three-stage research compressor which is now in construction. Computations for comparison were carried out with two different analysis codes.

Third International Conference on Inverse Design Concepts and Optimization in Engineering Sciences (ICIDES-III), Editor: G.S. Dulikravich, Washington D.C., October 23-25, 1991

FUNDAMENTAL EQUATIONS OF THE METHOD

Since inverse design strives for low loss flow without shocks and boundary layer separation, Prandtl's concept of distinct potential flow and boundary layer calculation is applied. In Fig. 1 the fundamental process of the method is sketched. The method computes the steady compressible potential flow in the passage between two blades of unknown shape from far upstream to far downstream on a stream surface of revolution. Besides the upstream and downstream velocity vector, the velocity distributions are prescribed along the arc length of the stagnation streamlines with their periodic parts in the upstream and downstream regions and along the blade suction and pressure sides. In this way velocity gradients can be prescribed, which is important for the boundary layer development and a prerequisite for loss minimization. Moreover, radius and thickness of the stream surface of revolution are prescribed along the axial coordinate. These boundary conditions are transformed by integration into the computation plane with stream function coordinates and their normals. The computation grid is rectangular in this plane and contour adapted in the physical plane. Therefore, no interpolations are necessary on the boundaries.

The equations of continuity and motion for steady, isentropic flow on a stream surface of revolution are

$$\frac{\partial\left(\rho\ h\ W_u\right)}{\partial\theta} + \frac{\partial\left(\rho\ h\ R\ W_m\right)}{\partial m} = 0 \tag{1}$$

$$\frac{\partial W_m}{\partial\theta} - \frac{\partial\left(R\ W_u\right)}{\partial m} = 2\ \omega\ R\ \frac{\partial R}{\partial m} \tag{2}$$

with the isentropic relation

$$\rho = f\ (W,\ \omega,\ R) \tag{3}$$

The appearance of a variable stream surface radius in the fundamental equations requires a different treatment of rotor and stator flows since in the relative system of the rotor an energy alteration is connected with a radius alteration. So the relative velocity W can no longer be prescribed by a potential. In the absolute system (following Vavra [3]) an equivalent potential φ_A can be defined by

$$\nabla\cdot\varphi_A = \vec{v}_A = \vec{w} + \vec{i}_1\omega\ R \qquad \text{and}\ \nabla\times\vec{v}_A = 0\ . \tag{4}$$

But the contour velocity distribution has to be prescribed in the relative system, thus one coordinate direction is given by the streamlines in the relative system. Together with the potential lines normal to the absolute velocity an oblique-angled coordinate system results, Fig. 2.

Third International Conference on Inverse Design Concepts and Optimization in Engineering Sciences (ICIDES-III), Editor: G.S. Dulikravich, Washington D.C., October 23-25, 1991

At velocities $W \ll \omega R$ and flow angles $\delta \approx \pi/2$ (e.g. in the stagnation point region) the angle α approaches zero so that both coordinate directions coincide. Following from numerical reasons this system consisting of an absolute potential and relative stream function is inconvenient for use as a computational grid.

The potential-streamfunction-plane is the computation plane of the inverse design method. Furthermore, for using it in the rotor the equation of motion is reduced to $\nabla \cdot \vec{w} = 0$. The consideration of the rotational character of the flow occurs by variation of the total quantities dependent on the stream surface radius. (Another consideration by definition of a transformed potential is published in [4,5].)

Since the critical sonic velocity is no longer constant, because of the variation of the total temperature, it is no longer applicable for normalization of the velocity like in the stator case. Hence, the upstream velocity W_1 is now applied for this purpose. The decision which difference operator for consideration of the type-dependence of the differential equation system has to be applied is taken by the magnitude of the local Mach number.

By transformation of the fundamental equations into the potential-streamfunction-plane and elimination of the flow angle the full potential equation follows [6]:

$$C_1 \cdot \frac{\partial^2 \ln W^*}{\partial \varphi^2} + C_2 \cdot \frac{\partial^2 \ln W^*}{\partial \psi^2} + C_3 \cdot \left[\frac{\partial \ln W^*}{\partial \varphi}\right]^2 + C_4 \cdot \left[\frac{\partial \ln W^*}{\partial \psi}\right]^2$$

$$+ C_5 \cdot \frac{\partial \ln W^*}{\partial \varphi} + C_6 \cdot \frac{\partial \ln W^*}{\partial \psi} + C_7 = 0$$

$$\text{with} \quad C_1 \ldots C_7 = f\,(W^*, \omega, R, h) \tag{5}$$

$$\text{and} \quad W^* = W/W_1 \quad \text{for the rotor}$$
$$= La \quad \text{for the stator}$$

The flow field is computed by the solution of the corresponding difference equation system applying relaxation combined with multi-grid. The change of type (elliptic-hyperbolic) from subsonic to supersonic flow regions depending on the sign of the coefficient C_1 is considered by modified difference equations. The transformation of the solution back into the physical plane is performed by integration of the equations of continuity and motion. It yields the field boundaries, i.e. the blade profiles and the cascade geometry.

For solving eq.(5) the dependence of the radius on the potential and stream function $R = f(\varphi, \psi)$ is necessary. Since only the axial development $R = f(z)$ is known by the prescription, this relation can only be discovered by an additional iteration in the course of the solution process. The radius distribution has to fulfill the condition of constant values in circumferential direction. Normally the same is true for the stream surface thickness. Moreover, the desired values of turning angle, pitch-chord ratio or blade thickness distributions are attainable by iterative variations of the prescribed boundary values (which are selfacting included in the code). The whole geometry of the problem is always the *result* of the computation and therefore completely unknown at the beginning.

CIRCULATION, LEADING EDGE RESOLUTION, SHOCKLESS DESIGN

The profile circulation necessary for the desired turning, follows from (s. Fig. 3):

$$\Gamma_P = \oint \vec{w}\cdot d\vec{s} - W_1\cdot\cos\beta_1\cdot\frac{2\pi R_1}{BN} + W_2\cdot\cos\beta_2\cdot\frac{2\pi R_2}{BN\cdot\Omega_{BW}} \qquad (6)$$

The line integral of the velocity along the computation grid boundary can be converted by the law of Stokes into an area integral

$$\oint \vec{w}\cdot d\vec{s} = -2\int \vec{\omega}\cdot d\vec{A} \quad . \qquad (7)$$

The rotational vector $\vec{\omega}$ indicates in axial direction, $d\vec{A}$ is perpendicular to the through-flowed area. For the stator $(\omega \equiv 0)$ and for a rotor with constant radius $(\vec{\omega} \parallel d\vec{A})$ the value of the line integral equals zero. Because of the reduction of the equation of motion this is also true for rotor flow with varying radius. The additionally existing circulation inside the computation grid is thereby neglected.

$$\oint \vec{w}\cdot d\vec{s} = 0 \qquad (8)$$

The profile circulation which is necessary for the actual turning problem and which should be rendered by the prescribed velocity distribution at the beginning of the design process is

$$\Gamma_P = \frac{2\pi\cdot R_1}{BN}\cdot\left[W_2\cdot\cos\beta_2\cdot\frac{R_2}{R_1}\cdot\frac{1}{\Omega_{BW}} - W_1\cdot\cos\beta_1\right] \qquad (9)$$

The circulation inside the computation grid neglected in the rotor case with varying radius can be estimated in maximum if the flow conus area divided by the blade number (i.e. vanishing profile area) is assumed as upper limit for the integration area:

$$\oint \vec{w}\cdot d\vec{s} = \frac{4\pi^2 n}{BN}\cdot\left(R_2^2 - R_1^2 \right) \qquad (10)$$

The relative deviation (refered to the circulation of the reduced equation of motion) is

$$\Delta\Gamma = \frac{-2\cdot\pi\cdot n\cdot R_1\cdot\left[\left(\frac{R_2}{R_1}\right)^2 - 1\right]}{W_1\cdot\left(-\cos\beta_1 + \cos\beta_2\cdot\frac{W_2}{W_1}\cdot\frac{R_2}{R_1}\cdot\frac{1}{\Omega_{BW}}\right)} \tag{11}$$

In the case of compressor cascades ($\beta_1 \geq 90^\circ$) the reduced equation of motion yields lower circulation for increasing stream surface ($R_2/R_1 > 1$) and higher circulation for decreasing stream surface. In standard cases the deviation amounts to less than 5 percent according to a turning angle deviation of less than 1 degree.

The leading edge region of a profile has special requirements for the numerical aspects of a computer program for calculation of the flow around an airfoil. In the design method this difficulty becomes especially clear since even the prescription data - the velocity distribution on the boundaries of the flow field to be computed - show the strong gradients in the stagnation point region (Fig. 4). This area can be recorded only insufficiently in an equidistant divided computation grid.

For appropriate resolution of the blade nose region it was found that the number of points on the flow field boundaries should be up to 2^4 or 2^5 times higher than that of the normal grid. Thereby local grid refinement is provided for the regions with steep gradients. For smaller point distances the possibility of emboxing of refinements was established. In a corresponding fitted arrangement a gradual transition of the mesh size follows. This is especially favourable for the accuracy of the solution. For even higher accuracy, a feedback calculation can be performed which uses the results of the fine grid for recalculation in the coarse grid in an iterative way with overlapping boundaries of both regions.

In case of velocity prescriptions on the boundaries of local supersonic regions an "ill-posed problem" is treated, i.e. no physical solution may exist. Numerically this often leads to the formation of oscillating shocks in the flow field, shown in Fig. 5. If they are weak enough, a provision for cancellation of these shocks is given in Fig. 6: Following the plotted characteristic directions in the supersonic region from the concerned region to the corresponding boundary values, these values can be modified for generation of additional expansion waves to remove the shocks [7].

RESULTS

The first example is a cascade for a compressor stator hub section with supercritical flow (local supersonic region on the suction side), Fig. 7. The high subsonic velocity $La_1 = 0.90$ is decelerated to the downstream value $La_2 = 0.593$ by a turning angle of 25 degrees and a relatively high pitch-chord ratio of $t/l_{ax} = 1.0$.

The stream surface radius R increases by 30 percent from upstream to downstream and the stream surface thickness h decreases by 25 percent in the same direction. Their prescribed slopes dependent on the axial length z are given in Fig. 8. The curves of the inner and outer radius of the stream surface of revolution consist of cosine slopes, the maximum angle of inclination of the stream surface is $\varepsilon = 25$ degrees. In the cascade region the stream surface thickness distribution follows a cubic parabola, in the upstream and downstream region it is calculated by constant flow area.

In the upper part of Fig. 7 the full line shows the prescribed velocity distribution on the blade suction and pressure side. This roof top distribution with maximum Mach number of 1.19 (La = 1.15) was chosen for separation-free flow with high loading. On the suction side transition takes place at the beginning of the pressure rise at 31 percent of chord length (at $Re = 4.7 \cdot 10^5$ and Tu = 4%).

In the lower part of Fig. 7 the computed profile shape is plotted. The dashed line marks the contour of the potential flow computation from which the manufacturing contour (full line) is derived by subtraction of the boundary layer displacement thickness (computed by Rotta's integral method [8]). The complete cascade geometry and the flow field characterized by the (full) lines of constant velocity (with the sonic line La = 1.0) are shown in Fig. 9. The cascade geometry data were used as input for the analysis code of Lücking [9]. The results, the contour velocity distribution (crosses in Fig. 7) and the velocity distributions in the flow field (dashed lines in Fig. 9) agree well with the distributions of the inverse code, even in the supersonic region.

Moreover, in Fig. 10 the course of the lines of constant radius (dashed-dotted), which can only be calculated iteratively (see above), coincide well with the demanded circumferential direction.

In Fig. 11 the prescribed velocity distribution of a rotor tip section (n = 3600 rpm) is plotted together with the resulting profile shape (both full lines). Despite of the low turning of 6 degrees, due to the high upstream velocity of La = 0.866 and the high pitch-chord ratio of $t/l_{ax} = 1{,}761$ the loading is high enough to require local supersonic flow on the suction side. In Fig. 12 the cascade geometry and the flow field consisting of lines of constant velocity is drawn, showing the great stagger of this design. The geometry of this result was again used to compute the velocity distributions for comparison by the finite volume method originating in P.W. McDonald [10]. The crosses in Fig. 11 and the dashed lines in Fig. 12 exhibit satisfying agreement with the design computation (full lines).

The velocity distribution of the rotor hub section (Fig. 13) belonging to the preceding rotor tip section was mainly influenced by a desired maximum thickness of the profile (in consideration of structural reasons). Therefore, high velocities appear on the suction and pressure side without high aerodynamic loading. The design on stream surface with radius increase of 14 percent (full line) is compared with plane flow design for equal upstream and downstream velocity vectors. It is to be seen that in the plane

Third International Conference on Inverse Design Concepts and Optimization in Engineering Sciences
(ICIDES-III), Editor: G.S. Dulikravich, Washington D.C., October 23-25, 1991

flow case higher circulation is needed for the same turning problem but a thinner profile results compared to the design on increasing radius. In Fig. 14 the cascade geometry is demonstrated and the isolines of the velocity are compared with the results of the finite-volume method [10]. In the front part of the flow channel including the local supersonic region the velocity field compares well. In the rear part, refering to a local aft-acceleration behind the supersonic patch the coincidence of the isolines is somewhat disturbed.

CONCLUSION

The present extended inverse method seems to be an effective procedure to design highly loaded axial compressor cascades on stream surfaces of revolution. It produces accurate results compared with complete flow field results of other methods and was successfully applied to cascade and multi-section compressor blade design.

[1] Schmidt, E.: Computation of Supercritical Compressor and Turbine Cascades with a Design Method for Transonic Flows. Trans. ASME, J. Eng. Power, Vol. 102, Jan. 1980, pp. 68-74

[2] Schmidt, E., Berger, P.: Inverse Design of Supercritical Nozzles and Cascades. Int.J.Num.Meth.Eng., Vol. 22, No. 2, Feb. 1986, pp. 417-432

[3] Vavra, M.H.: Aero-Thermodynamics and Flow in Turbomachines. Wiley, New York, 1960

[4] Klimetzek, F., Schmidt, E.: Transonic Blade Design on Rotational Stream Surfaces. AGARD Conf. Proc. No.421, May 1987

[5] Schmidt, E., Klimetzek, F.: Inverse Computation of Transonic Internal Flows with Application for Multi-Point Design of Supercritical Compressor Blades. AGARD Specialist's Meeting Computational Methods for Aerodynamic Design (Inverse) and Optimization, Loen, Norway, May 22-23, 1989

[6] Grein, H.-D., Schmidt, E.: Ein Berechnungsverfahren für die Auslegung von Verdichterbeschaufelungen. MTZ Motortechnische Zeitschrift 51, Juni 1990, pp. 248-255

[7] Schmidt, E.: Inverse Methods for Blade Design, Controlled Diffusion Blading for Supercritical Compressor Flow. VKI-LS Transonic Compressors, Brussels 1988-03

[8] Rotta, J.-C.: FORTRAN IV-Rechenprogramm für Grenzschichten bei kompressiblen, ebenen und achsensymmetrischen Strömungen. DLR FB 71-51, Göttingen, 1971

[9] Lücking, P.: Numerische Berechnung der dreidimensionalen reibungsfreien und reibungsbehafteten Strömung durch Turbomaschinen. Dissertation, RWTH Aachen, 1982

[10] Happel, H.W.: Anwendung neuer Entwurfskonzepte auf Profile für axiale Turbomaschinen. MTU Techn. Bericht 78/54A, München, 1978

Third International Conference on Inverse Design Concepts and Optimization in Engineering Sciences (ICIDES-III), Editor: G.S. Dulikravich, Washington D.C., October 23-25, 1991.

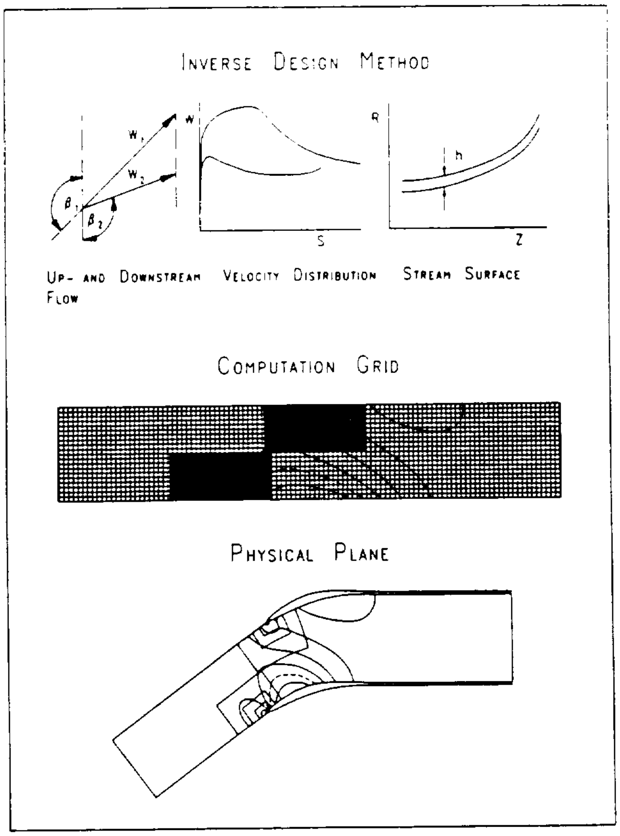

Fig. 1: Solution process of the inverse design method.

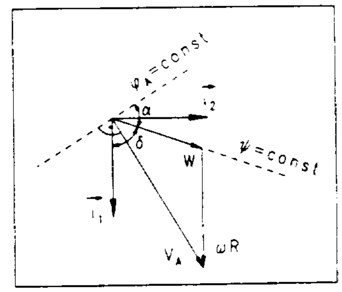

Fig. 2: Velocities and coordinate directions in an absolute potential/relative stream function system.

Calculation of Profile Circulation

circulation inside computation grid:

$$\Gamma = \int (\nabla \times \vec{w}) \cdot d\vec{A} = \oint \vec{w} \cdot d\vec{s}$$

stator, rotor with reduced equation of motion:

$$\nabla \times \vec{w} = 0 \quad \Rightarrow \quad \oint \vec{w} \cdot d\vec{s} = 0$$

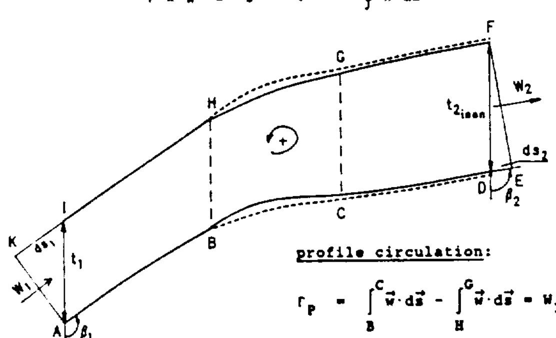

profile circulation:

$$\Gamma_p = \int_B^C \vec{w} \cdot d\vec{s} - \int_H^G \vec{w} \cdot d\vec{s} = W_1 \cdot t_1 \cdot \sin(\beta_1 - 90) + W_2 \cdot t_{2_{isen}} \cdot \sin(90 - \beta_2)$$

with

$$t = \frac{2\pi R}{BN}, \quad \frac{t_2}{t_{2_{isen}}} = Q_{BW}, \quad \sin(\beta - 90) = -\cos\beta :$$

$$\Gamma_p = \frac{2\pi R_1}{BN} \cdot W_1 \cdot \left[\frac{W_2}{W_1} \cdot \cos\beta_2 \cdot \frac{R_2}{R_1} \cdot \frac{1}{Q_{BW}} - \cos\beta_1 \right]$$

Fig. 3: Calculation of the profile circulation.

Third International Conference on Inverse Design Concepts and Optimization in Engineering Sciences (ICIDES-III), Editor: G.S. Dulikravich, Washington D.C., October 23-25, 1991.

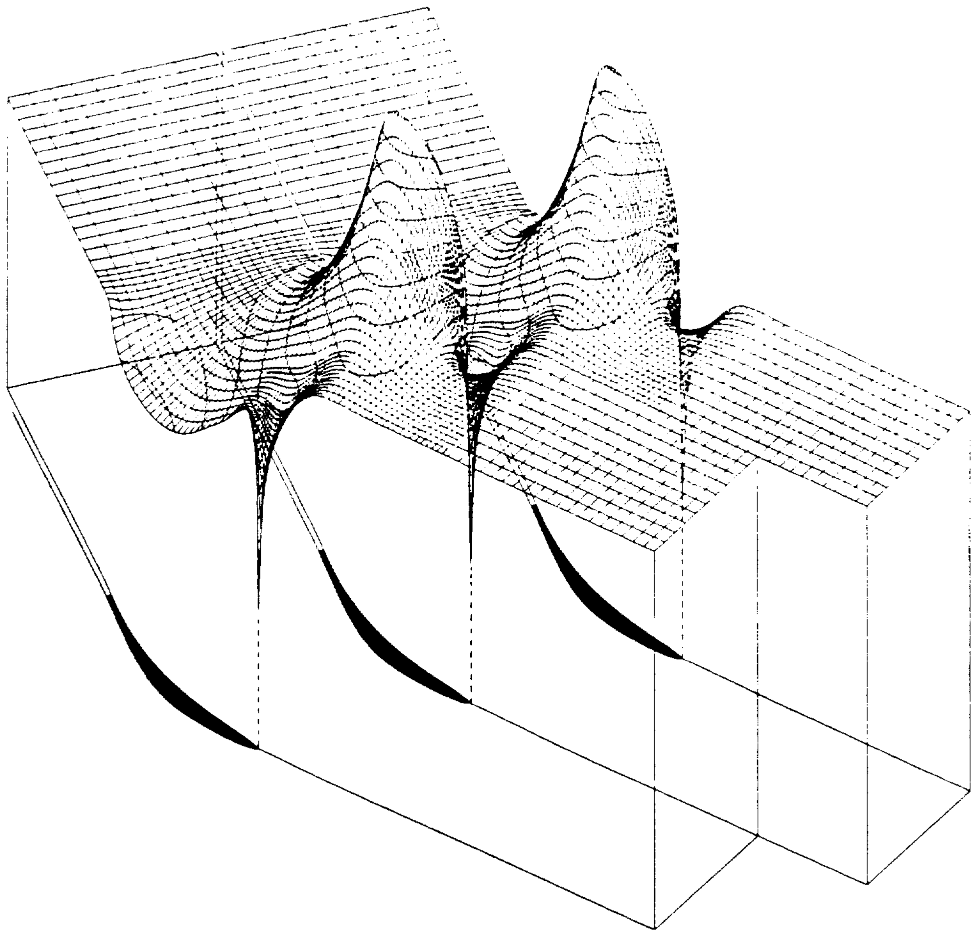

Fig. 4: Computation grid of a compressor cascade in the flow plane with velocity as height coordinate, demonstrating the resolution of of steep gradients in the stagnation point region.

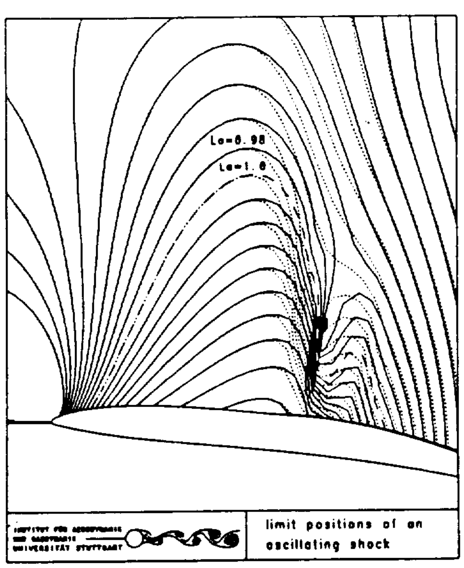

Fig. 5: Velocity fields and profile contours of a design with a shock for the limit positions of the oscillating shock.

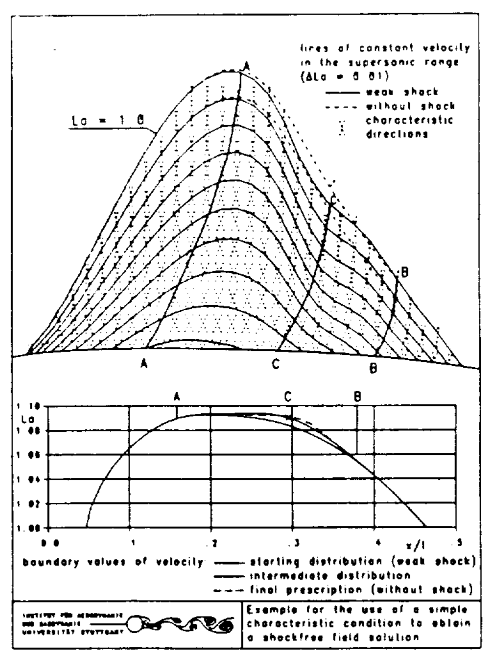

Fig. 6: Procedure for shockfree design.

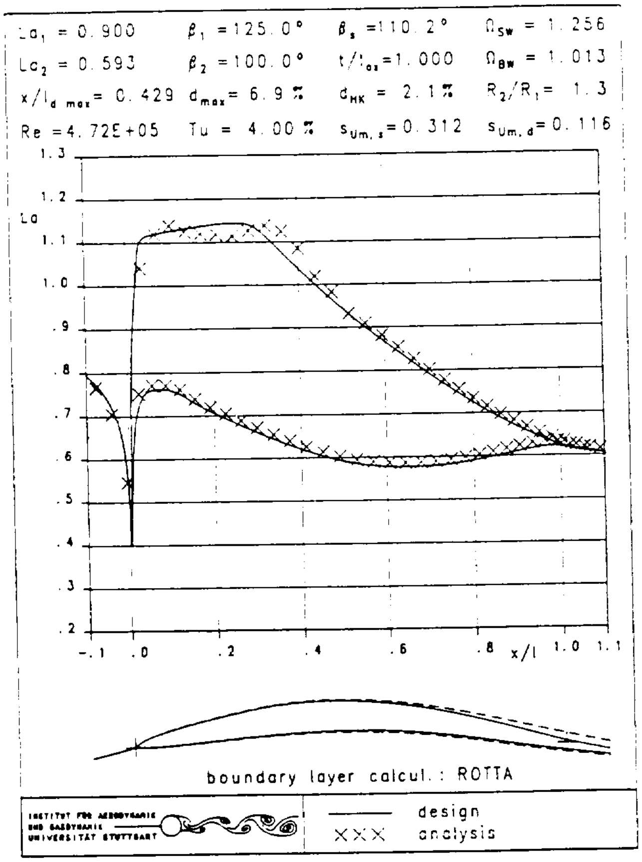

Fig. 7:

Comparison of Laval number distributions on the blade between design and analysis calculation on stream surfaces of revolution for the stator hub section. Additionally the potential flow contour (dashed line) and the metal section contour (full line) are indicated.

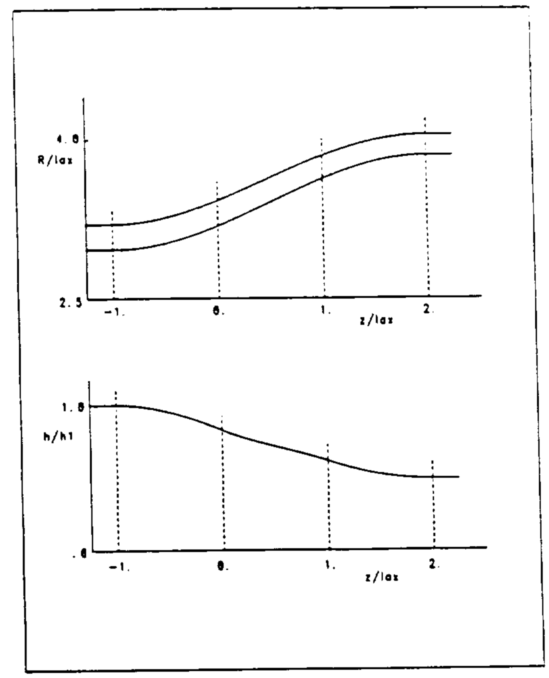

Fig. 8:

Slopes of inner and outer radius of the stream surface (top) and stream surface thickness (bottom) for the stator hub section.

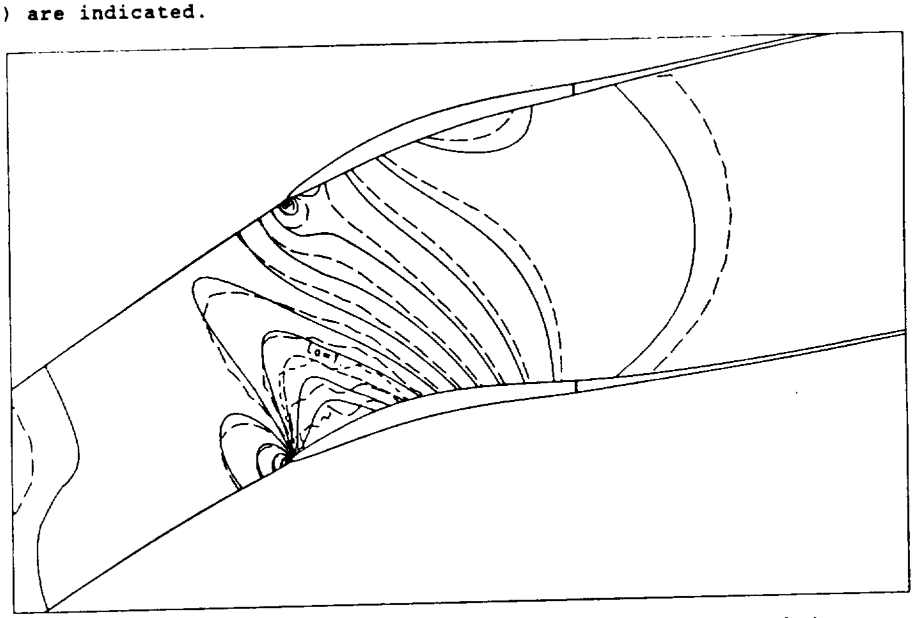

Fig. 9: Comparison of field distributions of Laval numbers between design (full line) and analysis calculation (dashed line) on stream surfaces of revolution for the stator hub section (increment ΔLa = 0.05, sonic line La = 1.).

Third International Conference on Inverse Design Concepts and Optimization in Engineering Sciences
(ICIDES-III), Editor: G.S. Dulikravich, Washington D.C., October 23-25, 1991.

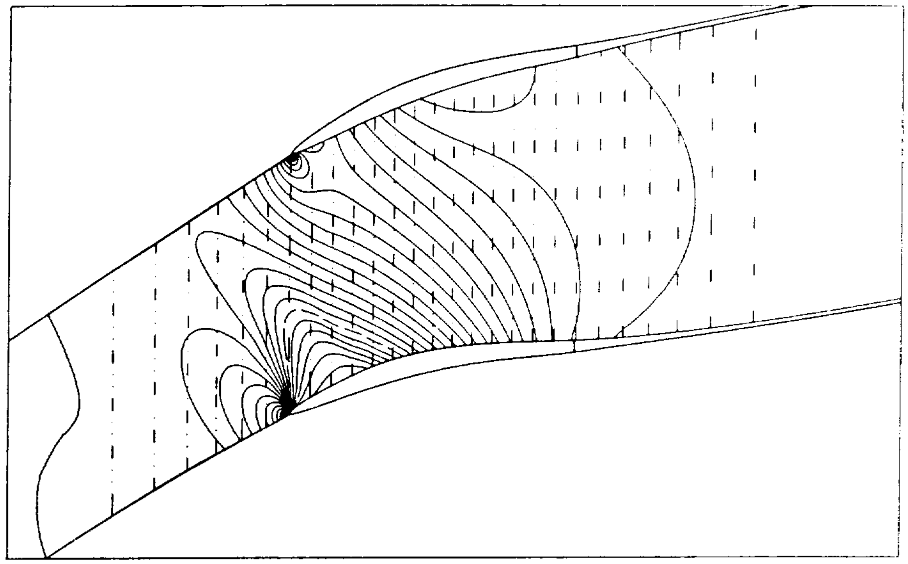

Fig. 10: Field distribution of Laval number (sonic line dashed, increment $\Delta La = 0.025$) and lines of constant stream surface radius (dashed-dotted) for the stator hub section.

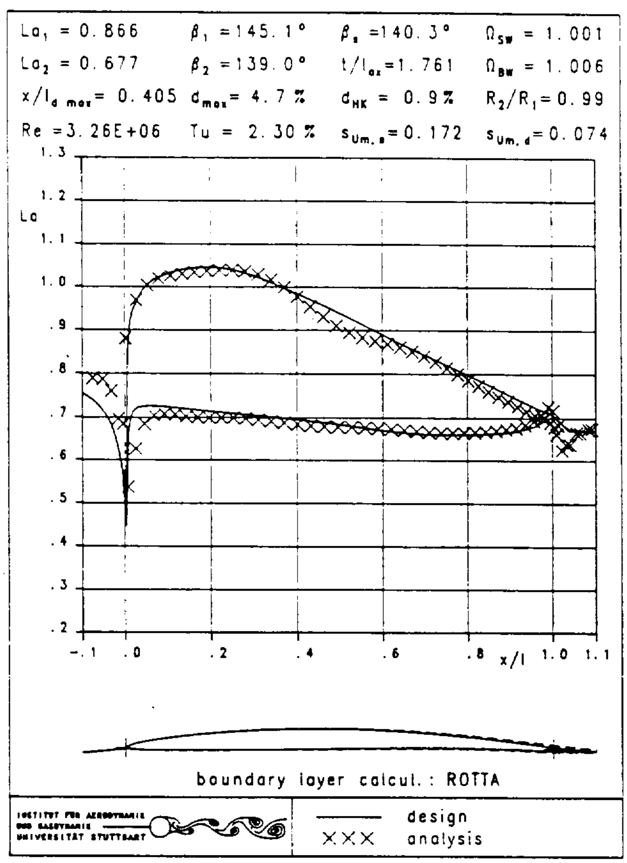

Fig. 11:

Comparison of Laval number distributions on the blade between design and analysis calculation on stream surfaces of revolution for the rotor tip section.

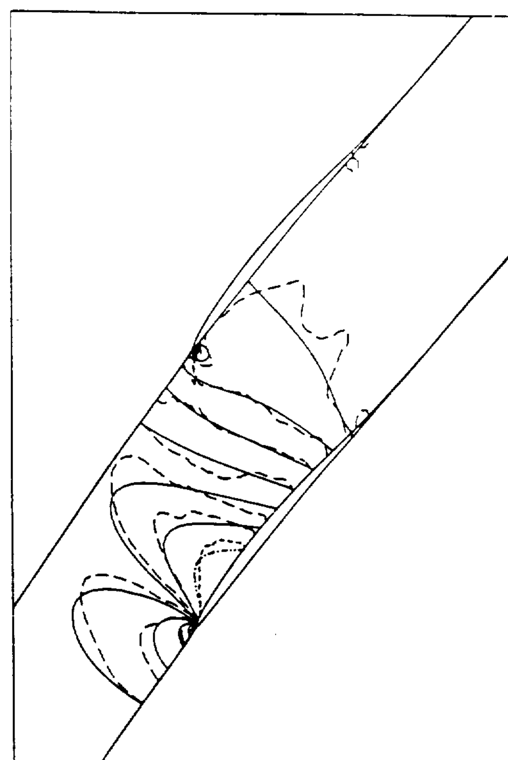

Fig. 12:

Field distributions of Laval number of design calculation (full line, sonic line dashed-dotted) and analysis calculation (dashed line, sonic line short dashed) for the rotor tip section (increment $\Delta La = 0.5$).

Third International Conference on Inverse Design Concepts and Optimization in Engineering Sciences (ICIDES-III), Editor: G.S. Dulikravich, Washington D.C., October 23-25, 1991.

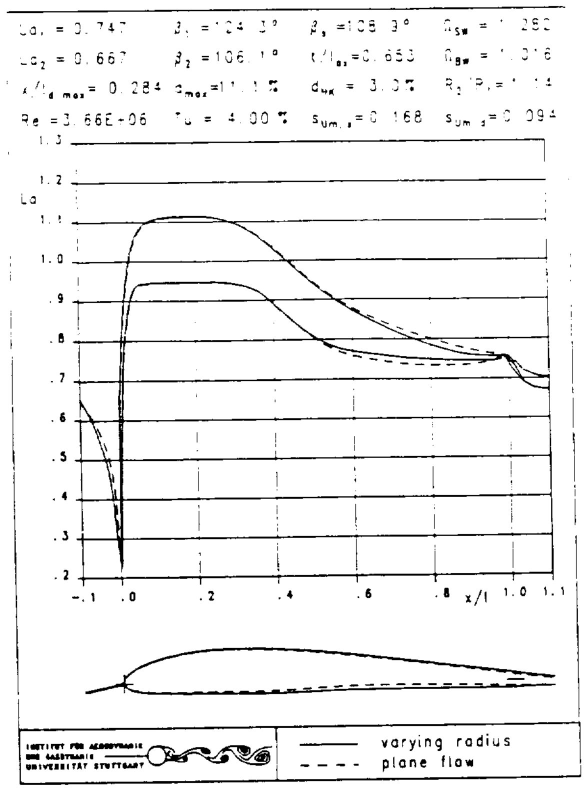

Fig. 13: Comparison of Laval number distributions on the blade and of blade contours between design of rotor hub section on plane stream surface (dashed line) and on stream surface of revolution (full line).

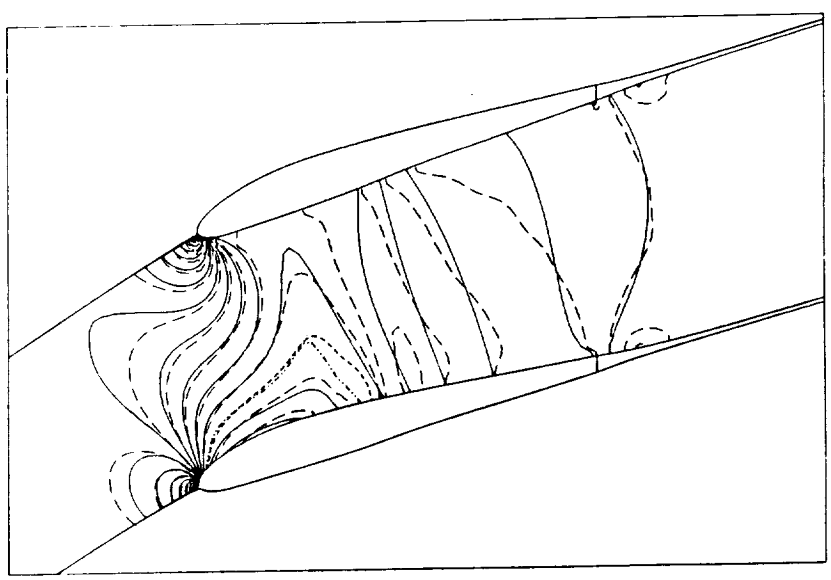

Fig. 14: Comparison of field distributions of Laval numbers between design (full line, sonic line dashed-dotted) and analysis calculation (dashed line, sonic line short dashed) on stream surfaces of revolution for the rotor hub section (increment $\Delta La = 0.05$).